Transform-Limited, Narrow-Linewidth Lasing Action in Organic Semiconductor Microcavities

V. Bulović, V. G. Kozlov*, V. B. Khalfin, S. R. Forrest

Lasing action in organic vertical-cavity surface-emitting laser (OVCSEL) structures is demonstrated. Optically pumped OVCSELs with an active layer composed of a thin-film organic semiconductor tris-(8-hydroxyquinoline) aluminum (Alq_3) doped with DCM laser dye produced very narrow linewidth (0.2 ± 0.1 angstrom), high-power (3 watts) emission that could be varied in different devices from orange to red. The efficient energy transfer from Alq_3 to DCM results in a threshold input energy of 300 microjoules per square centimeter. An operational lifetime $>10^6$ laser pulses was achieved for a device operated well above threshold in atmosphere. The linewidths above threshold are Fourier transform–limited and could potentially be narrowed further.

The recent interest in lasing action and stimulated emission in optically pumped thin films of small molecular weight organic semiconductors and polymers (*1*–*5*) is opening the door to a new generation of light-emitting organic devices: organic semiconductor lasers (OSLs). The low cost of organic materials and ability to grow them as quasi- and nonepitaxial thin films (*6*) facilitates integration of OSLs with other optoelectronic devices, making them attractive for a number of applications. The particular optical and electronic properties of organic semiconductors result in OSL performance (output power, differential quantum efficiency, and emission wavelength) that is significantly more temperature stable than conventional inorganic laser diodes (*2*), a potential advantage in optical communications and sensor applications. Furthermore, the short wavelength of optically pumped OSLs operating from 460 to 510 nm (*7*) is highly desirable for optical memory applications.

Demonstration of electrically rather than optically pumped OSLs is now the goal of much organic laser research. We have fabricated optically pumped OSLs with a slab waveguide structure that exhibited very low lasing thresholds (*1*). Electrical pumping of waveguide geometry OSLs, however, would require metallic contacts along the length of the guide and would also restrict the waveguide thickness to ~1000 Å because of low carrier mobilities in most organics. In such thin structures, absorption losses at the contact electrodes are very high, ultimately preventing laser action.

We have investigated an alternative geometry, an organic vertical-cavity surface-emitting laser (OVCSEL), where a thin organic film is sandwiched between two highly reflective mirrors. This structure provides a means for electrical pumping without increasing optical losses because the metal electrodes could also act as the cavity mirrors. Furthermore, in a microcavity OVCSEL, the total thickness of the organic films can be as small as $\lambda/2n$, which is only 1350 Å for a blue laser emitting at $\lambda = 460$ nm, with an organic film refractive index of $n = 1.7$. This thickness is comparable to those of efficient, low-voltage, electrically pumped organic light-emitting devices (*8*).

Amplified spontaneous emission (ASE) from a microcavity structure such as that used in an OVCSEL can be easily confused with lasing (*9*) because ASE is characterized by a narrow linewidth (typically a few nanometers) due to spectral filtering and is spatially confined to a collimated beam because of the directional nature of the output emission from the cavity. Nevertheless, a threshold in lasing output power, as well as significant spectral line narrowing above threshold, are readily observed in vertical-cavity semiconductor lasers (*10*).

In contrast to claims regarding the broad linewidth of polymer lasers (*3*, *4*), the linewidth of small molecule–based OVCSEL emission above the threshold is 0.2 ± 0.1 Å limited by the temporal characteristics of the laser emission; that is, the linewidth is Fourier transform–limited. We also present an estimate of the theoretical limit to the OVCSEL laser linewidth, which we find comparable to that of inorganic laser diodes. We measured operational lifetime that exceeded 10^6 pump laser pulses (more than 7 hours of operation).

The active layer consists of a 500-nm-thick Alq_3 film doped with 3% (by weight) of DCM, co-deposited in high vacuum (5×10^{-7} torr) by thermal evaporation onto the surface of a distributed Bragg reflector (DBR) dielectric mirror stack (Fig. 1). The 3% DCM concentration in Alq_3 was chosen because it previously yielded the lowest thresholds in slab-waveguide geometry OSLs (*2*). On top of the active layer, a 20-nm-thick Alq_3 buffer layer and a 200-nm-thick Ag mirror were sequentially deposited. The Alq_3 buffer layer reduces the DCM exciton quenching at the organic-metal interface. The DBR stack has a reflective stop band between 600 and 700 nm (reflectivity $R_2 = 0.995$), and the reflectivity of the Ag mirror is calculated to be $R_1 = 0.91$.

The lasers were optically pumped with a nitrogen laser ($\lambda = 337$ nm) that generated 500-ps pulses at a 50-Hz repetition rate. The pump beam was incident through the DBR stack, which had 80% transmission at $\lambda = 337$ nm, and was focused onto a circular, 100-μm-diameter spot on the organic film surface. The emission spectrum in the substrate normal direction (15° full-angle acceptance cone) was analyzed by a spectrograph with a charge-coupled device camera.

The pump energy absorbed by the host (Alq_3) is nonradiatively transferred to the guest (DCM) molecule (*11*). The Alq_3 emission spectrum matches the DCM absorption spectrum and results in efficient Förster energy transfer between the molecules, so only a low concentration of guest molecules is needed. This low density of optically active states in turn reduces the threshold and increases the laser efficiency (*12*). Because of the large (~100 nm) Stokes shift between the absorption and emission in both Alq_3 and DCM, the gain spectrum of this guest-host system is well removed from the Alq_3 absorption band, which reduces the lasing threshold and increases the operation lifetime of the device.

The spontaneous emission spectrum of the Alq_3:DCM OVCSEL just below threshold (Fig. 2A) is modified by the microcavity effects, where the peak at $\lambda = 635$ nm corresponds to a cavity mode. At $\lambda < 600$ nm and $\lambda > 700$ nm, the spontaneous emission is filtered by the modulation in the DBR transmission spectrum and results in the broad

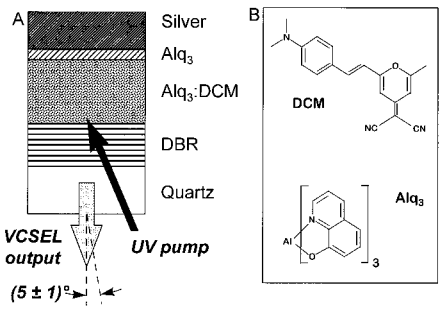

Fig. 1. (**A**) Laser structure showing 5 ± 1° output beam divergence and the experimental setup. (**B**) Chemical structural formulas of DCM and Alq_3.

Center for Photonics and Optoelectronic Materials (POEM), Department of Electrical Engineering and the Princeton Materials Institute, Princeton University, Princeton, NJ 08544, USA.

*To whom correspondence should be addressed: E-mail: kozlov@princeton.edu

satellite peaks observed. The spectrum above threshold, corresponding to an energy of E_{TH} = 300 μJ/cm^2, is completely dominated by the high gain, spectrally narrow laser emission (Fig. 2B).

Previous studies of slab waveguide Alq_3:DCM OSLs indicated tunability of the laser emission over a >40-nm-wide gain spectrum, as observed by varying the DCM concentration (*2*). This effect can also be used in the OVCSEL configuration. By changing the thickness of the active organic layers from d = 430 to 500 nm, we varied the laser emission from λ = 589 to 635 nm (Δλ = 46 nm). Because $n\,\Delta d/\Delta\lambda = (5/2)$, where n = 1.7 and Δd corresponds to the change in the thickness of the organic layers, we conclude that the optical cavity length is equal to $L = (5/2)\lambda/n$.

The dependence of the laser output power on input excitation (*13*) (Fig. 3) indicates a threshold at a pump energy density of E_{TH} = 300 μJ/cm^2. This threshold is two orders of magnitude greater than that for similar edge-emitting OSLs (*1*) as a consequence of higher optical losses in the microcavity structure and a short gain length (500 nm). We estimate the Alq_3:DCM material gain at threshold is $g_{TH} \gtrsim 1/(2nd)\ \ln(R_1R_2) = 650\ \text{cm}^{-1}$, which is comparable to the optical gain in InGaAs/GaAs quantum well structures (*10*). At a pump level of E = 30 mJ/cm^2, the peak output power was as high as 3 W for a device lasing at λ = 620 nm, and a collimated beam of laser emission was observed emerging from the device surface, with a 5 ± 1° divergence angle away from the normal (Fig. 1A). The highest pump energies caused some degradation in device performance because of damage to the Ag mirror.

Most of the measurements were performed in dry nitrogen, but we also studied OVCSEL operational lifetime under ambient conditions. The OVCSEL structure encapsulates the thin organic layer sandwiched between the dielectric mirror and the 200-nm-thick Ag layer. Figure 3 (inset) shows the laser output energy operating at $r = E/E_{TH}$ = 6 (where E_{TH} is the pump laser energy at threshold) as a function of time, or equivalently, the number of pump laser pulses. Surprisingly, the output power increased by almost 100% in the first hour of operation, which is probably related to optically induced changes at the organic layer/Ag interface that increased mirror reflectivity. However, slow degradation of the device became apparent after 4.5 hours (8×10^5 pump laser pulses). The operational lifetime of $>10^6$ pump laser pulses exceeds that of single-component dye lasers (*14*) by two orders of magnitude and is entirely related to the indirect excitation of dye molecules through nonradiative Förster energy transfer from the host material.

High-resolution emission spectra from the OVCSEL at increasing excitation levels (Fig. 4) show the transition from the 12 Å full-width spontaneous emission peak spectrally filtered by the microcavity below threshold to a resolution-broadened spectral line due to laser emission above threshold. The spectral width of the peak below threshold is related to the finesse of the microcavity (*15*), with additional broadening due to the presence of several transverse modes. Mode competition above threshold confines lasing to only a few of the transverse modes, leading to a concomitant reduction in the emission linewidth. Figure 4 (left inset) shows a 0.4 ± 0.1 Å broad emission line of an OVCSEL with d = 475 nm. Accounting for the 0.2 ± 0.1 Å instrument resolution, the Gaussian full-width at half-maximum of the lasing line is calculated to be 0.2 ± 0.1 Å.

Time evolution of OVCSEL emission studied with a streak camera (Hamamatsu C4780, 20-ps time resolution) shows the 40-ps output emission pulse just above threshold (E = 1.2 E_{TH}), where the pump pulse duration is 500 ps (Fig. 5A). The temporal behavior at E = 2.5 E_{TH} (Fig. 5B) indicates the presence of relaxation oscillations typical for lasers with a mismatch between the photon lifetime in the optical cavity, t_c (t_c = 100 fs in our case), and the spontaneous lifetime of the laser material, τ (τ = 5 ns for DCM in solution). The frequency of relaxation oscillation is $f_m = (1/2\pi)[(r-1)/(t_c\tau)]^{1/2}$. We

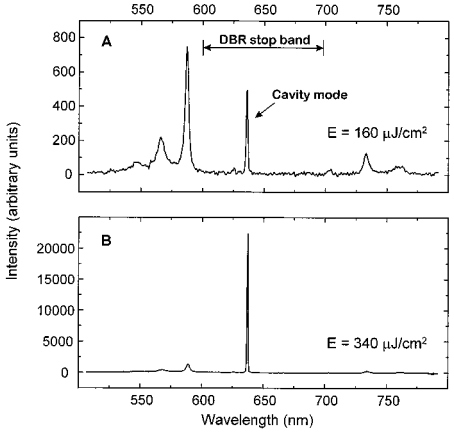

Fig. 2. (**A**) Spontaneous emission spectrum in the substrate normal direction from an Alq_3:DCM vertical-cavity surface-emitting laser with a 500-nm-thick active region in a (5/2)λ/n cavity modified by microcavity effects. A cavity mode is observed at λ = 635 nm. (**B**) Emission spectrum from the same OVCSEL at a high excitation level.

Fig. 3. Dependence of output energy on the input pump energy near threshold for an Alq_3:DCM vertical-cavity surface-emitting laser operating at λ = 635 nm. (**Inset**) Output power dependence on the number of pump pulses or equivalently time, with E = 2 mJ/cm^2, for an OVCSEL operating at λ = 620 nm.

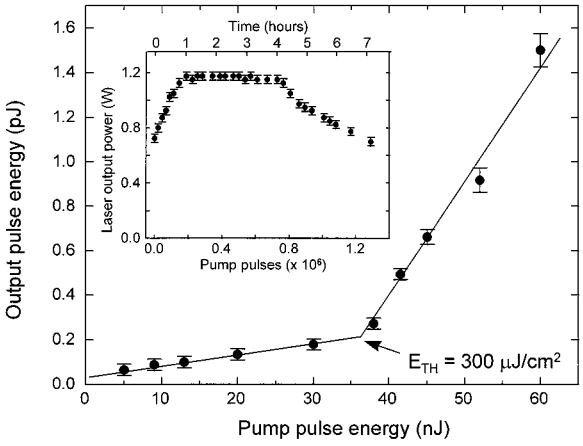

Fig. 4. High-resolution emission spectrum from a Alq_3:DCM vertical-cavity surface-emitting laser with a 500-nm-thick active region. (**Left inset**) Device with 475-nm-thick active region, and an instrument resolution broadened linewidth of 0.2 ± 0.1 Å in a (5/2)λ/n cavity as a function of excitation near threshold. Pump energies and the spectral full width at half-maximum are indicated. (**Right inset**) Calculated spectral dependence of the linewidth enhancement factor α.

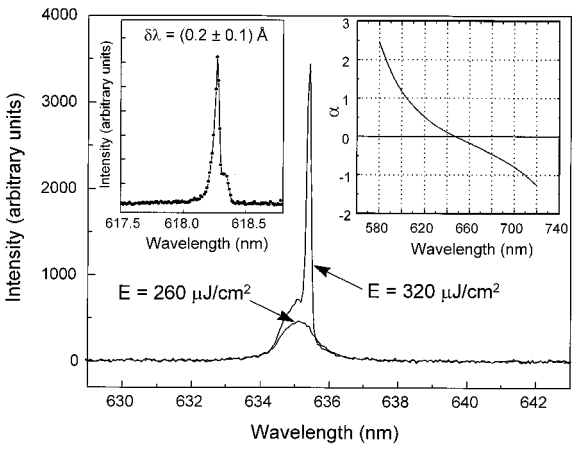

calculate that the oscillation period is $T = 1/f_m = 100$ ps, which matches the time delay between relaxation peaks in Fig. 5B. The transform-limited linewidth resulting from 40-ps pulses is $\Delta\lambda = 0.2 \pm 0.1$ Å, which matches the measured spectral linewidth of the OVCSELs.

The ultimate limit for the linewidth can be calculated from conventional semiconductor laser theory through the use of (*16*):

$$P\Delta\nu = \frac{h\nu g_{TH} n_{sp} \nu_{g0}^2 \xi^2}{16\pi d} \left[\frac{(\sqrt{R_1} + \sqrt{R_2})(1 - \sqrt{R_1 R_2})(1 - R_1)}{R_1 \sqrt{R_2} \ln(1/\sqrt{R_1 R_2})} \right] (1 + \alpha^2) \quad (1)$$

Here $\nu_{g0} = c/n$, where c is the speed of light in vacuum. The Bragg reflector and buffer layer act as the external cavity of total length $L = (5/2)\,\lambda/n \approx 930$ nm for $\lambda = 635$ nm, and the fraction of the mode in the active region is approximately $\xi = 0.5$. Also, $\alpha = \Delta n/\Delta n'$ is the linewidth enhancement factor, where Δn and $\Delta n'$ correspond to changes in the real and imaginary parts of the refractive index, respectively, due to the change in carrier density upon optical excitation. Finally, $n_{sp} = N_1/(N_1 - N_0)$, where N_1 and N_0 are the populations of the excited and ground states, respectively.

The linewidth of OSLs is comparable to that of inorganic semiconductor lasers with similar mirror reflectivities. A guest-host molecular system such as Alq_3:DCM can be treated as a four-level system, for which $n_{sp} = 1$ because the lower state involved in the radiative transition is unoccupied ($N_0 = 0$), whereas in inorganic semiconductors n_{sp} is typically near 2 or more (*16*). The main reduction in the linewidth of OSLs, however, is related to the α-parameter, which is well below 1 over a wide spectral range for materials such as Alq_3:DCM, whereas α ranges from 2 to 5 for most inorganic semiconductor lasers (*16*). We have estimated α (Fig. 4, right inset) by calculating $\Delta n'$ from the spontaneous emission spectrum using the Einstein relation (*17*), and Δn from $\Delta n'$ using the Kramers-Kronig relation. Because the spontaneous emission spectrum is broad and almost symmetric, α is small in the wavelength region centered near the emission peak, with $\alpha = 0.2$ at $\lambda = 635$ nm. In comparison to inorganic semiconductor lasers, OSLs have a larger ν_{g0} due to lower n, a larger g_{TH}, as well as a shorter d, all of which contribute to an increase in $P\Delta\nu$, thus partially offsetting linewidth-narrowing effects due to a small α. The power-linewidth product from Eq. 1 is then $P\Delta\nu = 1$ GHz mW, comparable to that of inorganic semiconductor lasers. However, the small Δn of OSLs implies a smaller chirp (narrower pulse width) as compared to inorganic semiconductor lasers.

Optical gain in vacuum-deposited organic thin films is sufficient for obtaining very high output power, optically pumped vertical-cavity surface-emitting lasers. Using these structures in an electrically pumped configuration will require reducing the lasing threshold of 300 μJ/cm^2 to values near 0.1 μJ/cm^2, assuming a pulsed peak pump current of ~1 kA/cm^2. The use of a higher top contact reflectivity or more optically efficient organic systems (*5*) may help realize this goal.

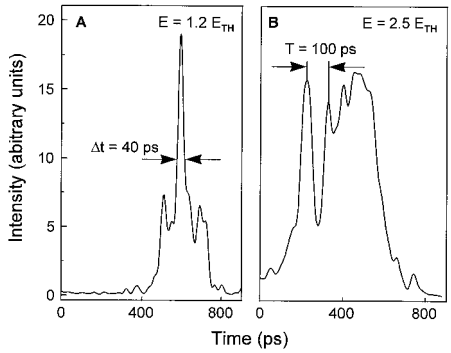

Fig. 5. Normalized temporal behavior of OVSCEL emission at excitation levels of (**A**) $E = 1.2\,E_{TH}$ and (**B**) $E = 2.5\,E_{TH}$, indicating the presence of relaxation oscillations of 40-ps duration at 100-ps intervals.

REFERENCES AND NOTES

1. V. G. Kozlov, V. Bulović, P. E. Burrows, S. R. Forrest, *Nature* **389**, 362 (1997).
2. V. G. Kozlov, V. Bulović, S. R. Forrest, *Appl. Phys. Lett.* **71**, 2575 (1997).
3. N. Tessler, G. J. Denton, R. H. Friend, *Nature* **382**, 695 (1996).
4. M. A. Díaz-García *et al*., *Appl. Phys. Lett.* **70**, 3191 (1997).
5. M. Berggren, A. Dodabalapur, R. E. Slusher, Z. Bao, *Nature* **389**, 466 (1997).
6. S. R. Forrest, P. E. Burrows, E. I. Haskal, F. F. So, *Phys. Rev.* ***B*** **49**, 11309 (1994); S. R. Forrest, *Chem. Rev.* **97**, 1793 (1997).
7. V. G. Kozlov, G. Parthasarathy, P. E. Burrows, S. R. Forrest, *Appl. Phys. Lett.* **72** (12 January 1998), p. 144.
8. P. E. Burrows *et al*., *J. Appl. Phys.* **79**, 7991 (1996).
9. G. J. Denton, N. Tessler, M. A. Stevens , R. H. Friend, *Adv. Mater.* **9**, 547 (1997).
10. L. A. Coldren and S. W. Corzine, *Diode Lasers and Photonic Integrated Circuits* (Wiley, New York, 1995).
11. M. Pope and C. E. Swenberg, *Electronic Processes in Organic Crystals* (Oxford Univ. Press, Oxford, UK, 1982).
12. F. P. Schafer, *Dye Lasers* (Springer-Verlag, Berlin, 1977).
13. The OVCSEL and pump laser power was measured with a large-area detector connected to Molectron EPM 1000 energy/power meter.
14. A. Costela, I. Garcia-Moreno, J. M. Figuera, F. Amat-Guerri, R. Sastre, *Appl. Phys. Lett.* **68**, 593 (1996).
15. Finesse is defined as the ratio of microcavity-mode spacing to a single-mode linewidth.
16. C. H. Henry, *J. Lightwave Technol.* ***LT*****-4**, 288 (1986).
17. See, for example, M. Weissbluth, *Atoms and Molecules* (Academic Press, New York, 1978).

18. We are grateful to the Air Force Office of Scientific Research (C. Lee and M. Prairie), the National Science Foundation Materials Research Science and Engineering Center, and the Universal Display Corporation for support of this work.

14 October 1997; accepted 5 December 1997

Accelerating Invasion Rate in a Highly Invaded Estuary

Andrew N. Cohen* and James T. Carlton

Biological invasions are a major global environmental and economic problem. Analysis of the San Francisco Bay and Delta ecosystem revealed a large number of exotic species that dominate many habitats in terms of number of species, number of individuals and biomass, and a high and accelerating rate of invasion. These factors suggest that this may be the most invaded estuary in the world. Possible causes include a large number and variety of transport vectors, a depauperate native biota, and extensive natural and anthropogenic disturbance.

Over the past few centuries, thousands of species of freshwater, estuarine, and marine organisms have dispersed outward from their native regions through human-mediated transport and have established sustaining populations in distant parts of the globe (*1*, *2*). Many of these organisms have profoundly affected the abundance and diversity of native biota in the regions they have invaded (*3*, *4*), and in some cases they have had substantial economic impacts (*5*). Despite these many invasions, data sets suitable for analysis of spatial or temporal patterns of aquatic invasions are rare. Here, we analyzed a synthesis of such data for one of

A. N. Cohen, San Francisco Estuary Institute, 1325 South 46 Street, Richmond, CA 94804, USA.
J. T. Carlton, Maritime Studies Program, Williams College–Mystic Seaport, Post Office Box 6000, Mystic, CT 06355, USA.

*To whom correspondence should be addressed. E-mail: acohen@sfei.org